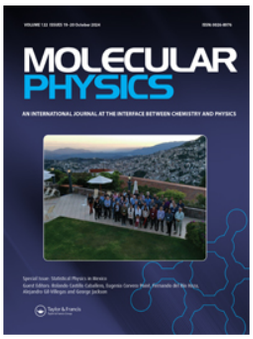

Taylor & Francis
Taylor & Francis Group

Molecular Physics

An International Journal at the Interface Between Chemistry and Physics

ISSN: (Print) (Online) Journal homepage: www.tandfonline.com/journals/tmph20

Isothermal compressibility and water self-diffusion coefficient in supercooled salt aqueous solutions using the Madrid-2019 model

L. F. Sedano, C. Vega & E. G. Noya

To cite this article: L. F. Sedano, C. Vega & E. G. Noya (22 Oct 2024): Isothermal compressibility and water self-diffusion coefficient in supercooled salt aqueous solutions using the Madrid-2019 model, Molecular Physics, DOI: 10.1080/00268976.2024.2418311

To link to this article: https://doi.org/10.1080/00268976.2024.2418311

Published online: 22 Oct 2024.

MOLECULAR PHYSICS e2418311
https://doi.org/10.1080/00268976.2024.2418311

Taylor & Francis
Taylor & Francis Group

RULL-ABASCAL SPECIAL ISSUE FOR STATISTICAL PHYSICS IN SPAIN (BY INVITATION ONLY) OPEN ACCESS Check for updates

Isothermal compressibility and water self-diffusion coefficient in supercooled salt aqueous solutions using the Madrid-2019 model

L. F. Sedano [a], C. Vega [a] and E. G. Noya [b]

[a]Departamento Química Física I (Unidad Asociada de I+D+i al CSIC), Fac. Ciencias Químicas, Universidad Complutense de Madrid, Madrid, Spain; [b]Instituto de Química Física Blas Cabrera, Consejo Superior de Investigaciones Científicas (CSIC), Madrid, Spain

ABSTRACT

The isothermal compressibility and self-diffusion coefficient of water in Li^+, Na^+, K^+, Mg^{2+} and Ca^{2+} chloride and sulfate salts aqueous solutions is calculated by means of molecular simulations using the Madrid-2019 force-field, that uses TIP4P/2005 model for water and assigns scaled charges for ions. Our simulations predict that the isothermal compressibilities of these salts retain the anomalous behaviour of water, i.e. compressibility increases as temperature decreases, contrary to the behaviour of normal liquids. A maximum in the isothermal compressibility, analogous to that of pure water, is observed for some of the salt solutions. For the 1 m NaCl solution, simulations are performed at several pressures up to 1000 bar to estimate the location of the second critical point. We estimate that the liquid-liquid critical point is located at 190 K and 1000 bar, i.e. it is shifted to slightly higher temperatures and lower pressures with respect to the most accurate estimation of its location in pure TIP4P/2005 water (172 K and 1861 bar). Regarding the self-diffusion of water, all salts increase water mobility in the very supercooled regime (at temperatures within 200–230 K), with K_2SO_4 producing the largest increase in water mobility, while $MgCl_2$ and $MgSO_4$ are the least effective in enhancing the self-diffusion coefficient of water.

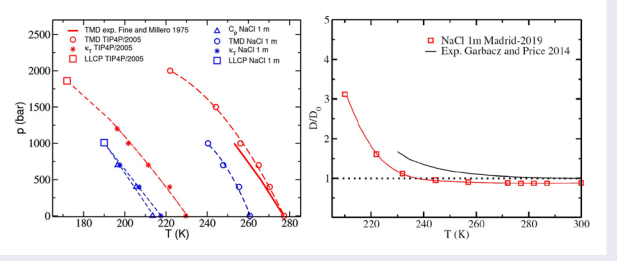

ARTICLE HISTORY
Received 30 July 2024
Accepted 11 October 2024

KEYWORDS
Electrolyte solutions; molecular dynamics; anomalous properties; liquid-liquid critical point; water self-diffusion coefficient

1. Introduction

Liquid water exhibits unusual behaviour in the supercooled regime. The maximum in density at 4°C (at room pressure) is the best-known anomaly, but there are many others. The isothermal compressibility, the isobaric heat capacity, the thermal expansion coefficient, the diffusion constant, the viscosity, the proton and oxygen spin relaxation time and dielectric relaxation time, all follow a power-law behaviour with temperature, suggesting an apparent singularity at −45°C [1,2]. These observations had led to the hypothesis of the existence of a second liquid-liquid critical point corresponding to a transition between a high density liquid (HDL) and a low density liquid (LDL), located in the high supercooled regime below the temperature of homogeneous ice nucleation [3], making its experimental identification challenging. According to this conjecture, the extrema in the above mentioned properties occur when the Widom line emanating from the critical point is crossed [4]. The existence of such second critical point is supported by the experimental observation of a seemly first-order phase transition between two glass states of water, known as high-density amorphous (HDA) and low-density amorphous (LDA) ices [5–7]. Further support comes from recent simulation studies that show that realistic models of water (TIP4P/2005 [8], TIP4P/ice [9], as well as the machine learning Deep Potential MD [10]) indeed present liquid-liquid phase separation, with the

CONTACT E. G. Noya eva.noya@iqf.csic.es Instituto de Química Física Blas Cabrera, Consejo Superior de Investigaciones Científicas (CSIC), Calle Serrano 119, Madrid 28006, Spain

critical point being located at about $T \sim$ 170–240 K and $p \sim$ 400–2600 bar, depending on the model potential [11–15]. For example, for TIP4P/2005 it appears at 172 K and 1861 bar [12] and for TIP4P/Ice at 188.6 K and 1725 bar [14].

Several strategies have been proposed to experimentally confirm the existence of this liquid-liquid critical point (LLCP). For example, by confining liquid water or using nanometric size droplets, it is possible to lower the crystallisation temperature [16]. Alternatively, it has also been shown that solutes can shift the critical point to higher temperatures and the homogeneous ice nucleation line to lower temperatures, facilitating the direct observation of the second critical point [17]. Diluted salt aqueous solutions have allowed to observe a transition between LDA and HDA with an associated volumetric change [18]. A few simulation studies have also addressed the effect of adding salt on water anomalies and the location of the LLCP [19–21]. Initial simulations using the TIP4P model for water and the Jensen and Jorgensen model, which assigns integer charges to the ions, indicate that a moderate concentration of NaCl shifts the critical point to higher temperatures and lower pressures [22]. A LLCP was also found in simulations (using the Madrid-2019 model, which assigns scaled charges to the ions, together with the TIP4P/2005 model for water) of a low concentrated LiCl solution, which again was located at slightly higher temperatures and lower pressures than in bulk water [23].

The addition of salt also changes the dynamic behaviour of water both at room conditions and in the supercooled regime. At normal pressure, the diffusion of pure water decreases by up to five orders of magnitude from room temperature down to 200 K [24,25]. Simulations using the E3B3 model, which reproduce this result, also predict that the diffusion constant exhibits a sigmoidal shape as the Widom line emanating from the second critical point is crossed, which becomes a discontinuity at pressures above the critical one [26].

Salts have been classified as 'structure breakers' or 'structure makers' depending on the change they effect on the self-diffusion of water: the latter induce a reduction of water mobility as concentration increases, whereas in the former, water self-diffusion first increases upon the addition of salt until it reaches a maximum before decreasing for high salt concentrations. However, this classification is not straightforward. For example, Kim and Yethiraj showed by simulations that NaCl acts as a structure maker at room temperature, but becomes a structure breaker at temperatures below freezing [27]. Further combined simulation and experimental studies on the diffusion of water in several electrolyte solutions at room temperature revealed the deficiencies of several model potentials in reproducing the experimental behaviour [28]. Whereas in experiments some salts induce a reduction of the self-diffusion of water, others, such as KCl, KBr, KI, CsCl, CsBr and CsI lead to an enhancement of water mobility. However, none of the considered model potentials (including two polarisable models) capture the increased diffusion of water in these salts. Using *ab initio* molecular dynamics simulations, Ding *et al.* were able to qualitatively reproduce the experimental findings, but with some quantitative differences [29], highlighting the need to incorporate the electronic degrees of freedom to capture the experimental behaviour.

Kann and Skinner [30] revisited the problem and, inspired by the works of Leontyev and Stuchebrukhov [31–33], assigned scaled charges to the ions. This scaling allows to incorporate in a implicit way the screening of the electric continuum: $q_{eff} = q/\sqrt{\epsilon_{el}}$, with ϵ_{el} being the high frequency dielectric constant. These authors demonstrated that the dependence of self-diffusion on salt concentration aligns with experimental results when scaled charges are assigned to the ions. This adjustment successfully recovers the enhanced diffusion of water observed for certain salts in experiments. A recent systematic study showed that scaled charges can be fitted to reproduce transport properties quite accurately but at the cost of loosing some accuracy on thermodynamic properties [34,35]. Following a different approach, which uses simple models that allow charge transfer between molcules [36], Yao *et al.* managed to reproduce the experimental water diffusion coefficient of NaCl and KCl solutions as a function of concentration at ambient conditions [37]. But it remains to be seen how charge transfer force-fields perform when dealing with thermodynamic properties, such as densities, solubilities, etc [38].

The use of scaled charges has been adopted by several research groups and is becoming increasingly widespread. Indeed, the recently proposed Madrid-2019 force-field [39,40] employs scaled charges and offers parameters for all alkaline and halogen ions in solution parameterised in conjunction with the TIP4P/2005 model for water. This force-field provides a rather good overall description of electrolyte solutions, reproducing fairly well the densities, viscosities and diffusion coefficients of salt solutions up to the solubility limit at room conditions [39]. It also captures the shift in the temperature of maximum density at low salt concentration [41,42], and the freezing point depression [43], among other properties. Still, it is important to recognise that a single parameterisation is unable to predict all the properties accurately [34,44]. In view of this, some authors suggest that further improvement will come from machine learned potentials [45,46]. Nevertheless, further

studies using simple potentials with scaled charges can provide valuable insights into the origin of their successes and failures which can be useful for further force-field development.

The main goal of this work is to investigate by computer simulation the effect of adding salt on the anomalous behaviour of supercooled salt solutions. As mentioned before, the anomalous behaviour of water might persist upon the addition of low concentrations of salts, and certain salts might even shift the LLCP to higher temperatures and lower pressures, facilitating its experimental verification. The study is performed using the Madrid-2019 force-field [39] in which water is modelled with TIP4P/2005 [8]. TIP4P/2005 reproduces reasonably well the properties of supercooled water [47]. TIP4P/2005 is able to capture the shift to lower temperatures of the maximum density and the isothermal compressibility maximum, as pressure increases [47–49]. It also reproduces rather well the dynamic behaviour, finding good agreement with experiments for the diffusion coefficient and viscosity [47,50]. Given the good overall performance of Madrid-2019 force-field, in this work, we explore the properties of supercooled salts solutions, focussing in particular, in the isothermal compressibility and in the self-diffusion coefficient of water. The shifts effected by the salts on the location of the isothermal compressibility (which defines the Widom line emanating from the LLCP) can be used to infer the location of the hypothetical LLCP. Our exploratory study of self-diffusion of water in supercooled salt solutions indicates that all the salts increase the diffusion of water at low temperatures. The enhancement in water mobility in salt solutions in the supercooled regime is corroborated by the few available experimental studies, but we hope that this article stimulates further experimental studies on this topic.

2. Simulation details

Molecular Dynamics simulations were performed with GROMACS [51]. The simulations were carried out in the *NpT* ensemble. Newton's equations of motion were integrated with a leap-frog algorithm using a time step of 2 fs. Temperature and pressure were controlled using the Nose-Hoover [52,53] thermostat and the Parrinello-Rahman [54] barostat, both with a relaxation time of 2 ps. Interactions between water molecules were described using the rigid non-polarisable TIP4P/2005 [8] and ions were modelled using the Madrid-2019 [39] force-field which was parameterised specifically for TIP4P/2005. A cutoff radius of 1 nm was employed for the dispersive and the real part of electrostatic interactions. Long range electrostatic interactions were taken into account using the Particle Mesh Ewald Method [55,56]. Standard long-range corrections to Lennard-Jones energies and pressures were applied [57]. The geometry of the water molecules was constrained using the LINCS [58] algorithm except when the system included the sulfate, in which case SHAKE [59] was used as it has been proven more efficient. The high symmetry of the sulfate anions poses some technical problems for the geometry constraint algorithms [40]. These can be avoided by treating sulfur as a massless atom and redistributing its mass on the remaining atoms of the ion. Thermodynamic properties are not affected by mass. The mass redistribution leads to a higher moment of inertia of the sulfate anion and, hence, to a lower rotational dynamics. However, since the total mass is conserved, we do not expect the translational dynamics to be significantly affected.

Simulations were performed in a cubic simulation box containing 555 water molecules and the corresponding number of ions to achieve 1 molal (i.e. 1 mol of salt per kg of water which corresponds in practice to 10 molecules of salt into 555 molecules of water) and 2 molal (corresponding to twenty molecules of salt) concentrations. Periodic boundary conditions were applied in the three directions of space.

The isothermal compressibility and self-diffusion of water in sodium, lithium, potassium, magnesium and calcium chloride and sulfate salts aqueous solutions at 1 m and 2 m concentrations were calculated over a broad range of temperatures, down to about 200 K. Notice that all simulations below 240 K are metastable with respect to crystalisation of water as the freezing temperature of the TIP4P/2005 model is 250 K, and for the solutions and concentrations of this work we expect decreases of about 4–8 K of the freezing temperature [43]. They are also likely to be metastable with respect to salt precipitation at the lower temperatures and, some of them, even over the whole range of temperatures. Even though the solubility of these salts modelled with the Madrid-2019 model has only been calculated for NaCl at room pressure, some salts (K_2SO_4 and $CaSO_4$) are known to be very poorly soluble at room conditions. However, we did not observe either ice formation or salt precipitation, as these are activated processes that must overcome a free energy barrier.

The isothermal compressibility is defined as:

$$\kappa_T = \frac{1}{\rho}\left(\frac{\partial \rho}{\partial p}\right)_T \tag{1}$$

It is related to volume fluctuations in the isothermal-isobaric ensemble:

$$\kappa_T = \frac{\langle V^2\rangle - \langle V\rangle^2}{k_B T \langle V\rangle} \tag{2}$$

where $\langle V \rangle$ is the average volume of the system and k_B is the Boltzmann constant. We used the fluctuation formula Equation (2) to obtain κ_T. Rather long simulations were needed to reduce statistical errors in the estimation of κ_T. Typically, simulations are run by hundreds of ns at the higher temperatures ($T \gtrsim 240$ K) and up to 3 μs at the lower temperatures ($T \lesssim 240$ K). We checked that at the lower temperatures, water molecules diffuse a distance larger than its molecular diameter over a period of 100 ns, which is a requirement that ensures that a reasonable sampling is achieved in our simulations.

The self-diffusion of water in the salt solutions was estimated using the Einstein relation:

$$D = \lim_{t\to\infty} \frac{1}{6t} \left\langle \frac{1}{N} \sum_{i=1}^{N} [\mathbf{r}_i(t) - \mathbf{r}_i(0)]^2 \right\rangle \qquad (3)$$

where $\mathbf{r}_i(t)$ and $\mathbf{r}_i(0)$ are the vector positions of the water molecule i (taken as the vector position of the oxygen) at time t and at the initial time, N is the number of water molecules, and the brackets denote an ensemble average. The diffusion coefficient was estimated from a linear fit of the mean squared displacement (MSD), averaged using multiple time origins along the simulations, as a function of time. For temperatures above 215 K, the linear fit was typically done after 2 ns, whereas for $T \lesssim 215$ K after 10 ns was taken to ensure that the diffusive regime had already been established. Previous simulations have shown that, at low temperatures, the mean square displacement of water exhibits a plateau region between the ballistic and diffusive regimes, caused by the fact that, at low temperatures, water molecules need more time to escape from their neighbour cages [60]. Further details about this issue are given in Section 3.3.

It is well known that the estimation of the diffusion coefficient by simulations is affected by finite-size effects [61]. Yeh and Hummer proposed an analytical expression to account for this effect [62]. However, since the viscosity of the solution as a function of temperature needs to be known to calculate such correction, and considering the wide range of thermodynamic states studied in this work, we have evaluated the outreach of system size effects for three systems containing 555, 2220 and 4440 water molecules (N_w) for NaCl at 298.15 K 1 m and 2 m. We found that for pure water and NaCl solutions, when the largest system is taken as a reference, the difference in diffusion for the smallest system is around 6 %, and about 1.5 % for the intermediate box. This might seem a non-negligible deviation. Nevertheless, throughout this work, we evaluate the relative water diffusion D/D_0, where D is the diffusion of water in the solution and D_0 stands for the self-diffusion of (pure) water. The evaluation of the relative diffusion shows deviations below 1.5 and 0.1 % for the systems $N_w = 555$ and $N_w = 2220$ respectively. Furthermore, since the size correction is directly proportional to the temperature and inversely proportional to the viscosity (which increases as T is lowered), we expect that the correction will actually be smaller at lower temperatures. Note that the low dependency of the ratio D/D_0 with the system size in salt solutions has been previously reported in the literature [28].

3. Results

3.1. Effect of pressure on the density and κ_T of a NaCl solution

The variation of the density with temperature of a 1 m NaCl solution along a few isobars within 1–1000 bar is shown in Figure 1(b). As already reported in our previous work [41], at room pressure the density exhibits a maximum at 260.7 K, which is in fairly good agreement with the experimental estimation (262.7 K). The values of densities are also very close to the measurements available for temperatures within 270–300 K [41]. The simulated density at room pressure exhibits a minimum at about 195 K. The existence of a minimum in the density of pure water has been reported in experiments [63] (of water confined in narrow pores) and in simulations using several water models (TIP4P/2005 [47], TIP4P/ice [14], TIP5P and ST2 models). TIP4P/2005 locates the minimum in density at 200 K at room pressure, i.e. the addition of 1 m of NaCl displaces the minimum by about 5 K, which is much lower than the shift of about 16 K in the temperature of maximum density (TMD).

The density of the 1 m NaCl solution increases with pressure and the TMD shifts to lower temperatures, from 260.7 K at room pressure to 240.4 K at 1000 bar. This gives a roughly constant shift of about 15–17 K with respect to the TMD of water for all pressures. The location of the TMD in the solution at different pressures is given in Table 1, together with that of pure TIP4P/2005 water. The Madrid-2019 provides fairly accurate results of the experimental densities, which are available only (at 400 bar and higher pressures) for $T > 273$ K. The minimum in density was only observed at room pressure. It is possible that this minimum still exists in the NaCl solution for $p > 400$ bar but at lower temperatures than those explored in this work. However, exploration of the configurational space becomes prohibitively expensive for temperatures below $T =$190–180 K due to the slow dynamics of the system.

The isothermal compressibility is shown in Figure 1(a). At temperatures above 273 K, the isothermal compressibility becomes lower as pressure increases both in pure

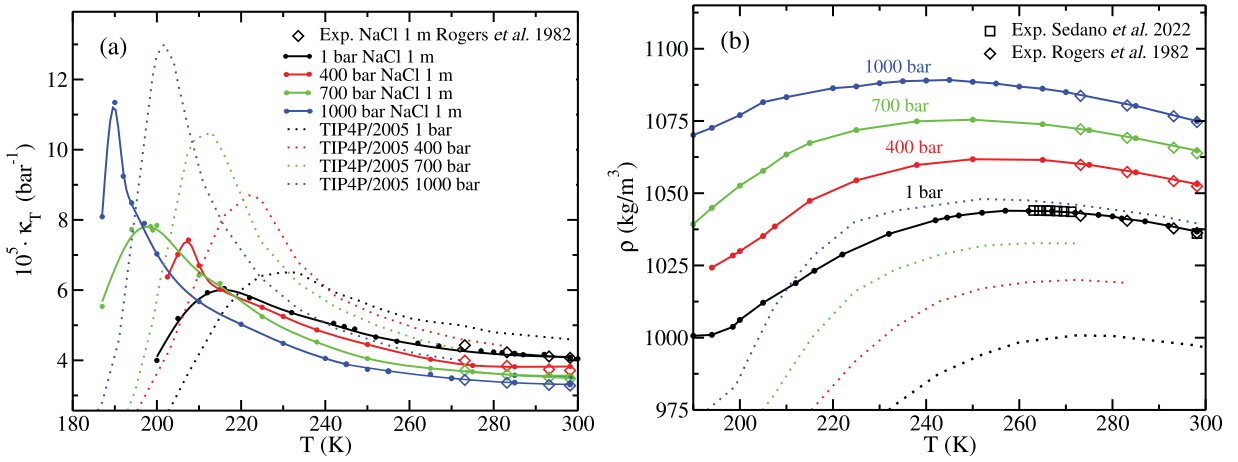

Figure 1. (a) Isothermal compressibility as a function of temperature along the 1, 400, 700 and 1000 bar isobars. For comparison, results for pure TIP4P/2005 water from Ref. [48] are also shown (dotted lines). Circle-filled lines: 1 m NaCl solutions (Madrid-2019); diamonds: experimental data from Ref. [64]. (b) Density of a 1 m NaCl solution as a function of temperature for the same isobars. Symbols are the same as in panel (a). Squares: experimental data from Ref. [41].

Table 1. Temperature of maximum density (TMD) and temperature of maximum κ_T (TMκ_T) as a function of pressure for TIP4P/2005 water and the 1 m NaCl solution simulated with the Madrid-2019 force-field.

	TMD (K)		TMκ_T (K)	
p (bar)	Water	1 m NaCl	Water	1 m NaCl
1	277.3	260.7	229.6	217.5
400	270.4	255.5	221.8	207.0
700	265.0	247.8	211.4	198.0
1000	256.2	240.4	201.7	190.0

water and in the salt solution. The magnitude of κ_T decreases with the addition of salt. At the same thermodynamic conditions κ_T is lower in the 1 m NaCl solution than in pure water. In this temperature regime, isothermal compressibilities obtained with the Madrid-2019 model are in very good agreement with the experimental measurements [64]. Moving now to the highly supercooled regime, at room pressure, the isothermal compressibility κ_T of pure TIP4P/2005 water exhibits a maximum at about 230 K that becomes more pronounced and shifts to lower temperatures as pressure increases. The location of the maxima at room pressure is in fairly good agreement with experiments, although the peak in the isothermal compressibility is about twice more pronounced in experiments than in the TIP4P/2005 model [14]. The 1 m NaCl solution exhibits a similar qualitative behaviour to that of pure water, but the maxima are shifted about 10 K to lower temperatures (see Table 1) and the magnitude of κ_T is lower in the 1 m NaCl solution as compared to that of pure water at temperatures above 273 K and at the maximum. Thus, in NaCl solutions at 1 m, the TMD is shifted by about 15 K with respect to that of pure water for pressures up to 1000 bar, but the maximum in compressibility determining the Widom line is shifted by a smaller amount (around 10 K).

The maxima in κ_T mark the location of the Widom line emanating from the second critical point, but, by itself, this line does not provide an estimation of the LLCP. With the aim of locating the LLCP in the 1 m NaCl solution, the maxima (along the isobars) in the isobaric heat capacity (C_p) are also drawn in Figure 2. Heat capacities were calculated from the fluctuations in the instantaneous enthalpy [57]. It is known that the C_p of water can only be properly described in simulations that explicitly incorporate nuclear quantum effects [65]. Thus, we do not expect a good agreement between the C_p provided by the Madrid-2019 force-field and experiments. Nevertheless, the maxima in C_p are useful to obtain an estimate of the LLCP in the salt solution, as the lines of maximum κ_T and C_p should converge at the critical point. Extrema in the response functions as the Widom line is crossed do not occur at the same thermodynamic conditions but they should merge at the critical point. As can be seen in Figure 2, both lines converge at $T = 190$ K and $p = 1000$ bar, i.e. the LLCP shifts by about 18 K to higher temperatures and by about 800 bar to lower pressures with respect to that of pure water (located at $T = 172$ K and $p = 1861$ bar [12]). This shift is qualitatively consistent with previous estimates for a 0.67 m NaCl solution derived from simulations with using the Jensen and Jorgensen force-field with integer charges in the ions and the TIP4P for water [20,22]. The shift predicted by Corradini *et al.* is similar in temperature (about 10 K) but significantly larger in pressure (about 2000 bar, occurring at negative pressures) than the shift predicted in this work using the Madrid-2019 force-field. It has been suggested in the literature that adding salt produces

changes in the hydrogen bond network of water similar to those observed by applying pressure [67,68]. However, this view has been recently challenged by simulations using machine learning force-fields (trained with *ab initio* calculations), which indicate that distortions caused by the ions are restricted to the first coordination shell and are different from those observed by applying pressure [69]. A detailed microscopic analysis of the effect of ions on the structure water is beyond the scope of this work. However, our results on the TMD and κ_T do not to support that the effect of salt is analogous to that of pressure. As can be seen in Figure 2, the shift in the TMD when adding 1 m NaCl of salt at room pressure is similar in magnitude to that observed by applying a 1000 bar pressure to pure water. However, the evolution of κ_T with temperature is significant different (see Figure 1(a)). The maximum of κ_T in pure water at 1000 bar occurs at lower temperatures than in the 1 m NaCl solution at room pressure, and the height of the peak is substantially higher in water at 1000 bar. Thus, our results also indicate that the parallelism between addition of salt and applying pressure should be taken with care.

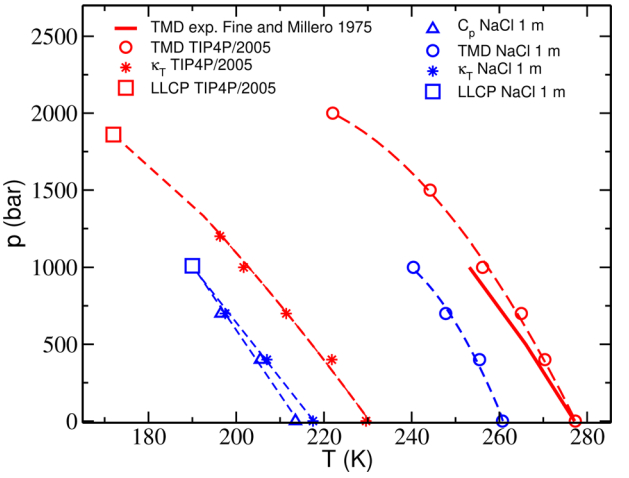

Figure 2. Pressure-temperature diagram showing the maximum isothermal compressibility and maximum density lines for pure water (red lines and red symbols) and a 1 m NaCl solution (blue lines and blue symbols). Dashed lines are fits to the simulation results. For the salt solution, the line of maximum heat capacity (C_p) is also drawn. The point at which the maxima in κ_T and C_p converge provides an estimate of the LLCP, marked by the blue square (190 K, 1000 bar). The red square signals the LLCP in TIP4P/2005 water (172 K, 1861 bar from Ref. [12]). Simulation results for pure water were taken from Ref. [48] and experimental data of the water TMD line were taken from Ref. [66].

3.2. Effect of chloride and sulfate salts on κ_T

The isothermal compressibility as a function of temperature at room pressure for various chloride and sulfate salts at 1 m and 2 m concentrations is shown in Figure 3.

Let us start by discussing the results at 1 m concentration. At temperatures above 273 K, all the chlorides lower κ_T, with the extent of this reduction correlating with the valency of the cations. Monovalent cations (Li^+, Na^+ and K^+) decrease κ_T by around 10%, whereas divalent cations (Mg^{2+} and Ca^{2+}) reduce it by about 15%. However, this trend does not hold for the sulfates. In this case, all the cations decrease κ_T by about 20%, regardless of their valency. For 1 m sulfate salts, the compressibility seems to follow a universal behaviour above 240 K regardless of the cation. The same is true for the 2 m sulfate solutions, although in this case the K_2SO_4 deviates somewhat from the universal behaviour. One possible explanation for the stronger dependence of κ_T on the cation in chloride salts compared to sulfate salts is that, due to the large size of the sulfate anion relative to the cations, the thermodynamic behaviour is primarily dominated by the sulfate anion, with the cations playing a secondary role. Further research is needed to confirm this hypothesis. For all 1 m salt solutions, κ_T exhibits an anomalous dependence on temperature. As in pure water, κ_T increases when the temperature decreases, contrary to what occurs in simple liquids. In the supercooled regime, κ_T exhibits a maximum for the majority of the salts. These maxima are shifted to lower temperatures compared to the maximum of κ_T in pure water. The exceptions are $CaCl_2$ and Li_2SO_4, for which a pronounced enhancement of κ_T is observed at the lower temperatures simulated, but not a maximum. If κ_T exhibits a maximum in those solutions, it is shifted to very low temperatures. The maximum value of κ_T is lower in the chloride salts than in pure water. This is specially evident for $MgCl_2$, which produces only a very mild peak around 235 K. However, in the sulfate salts, the opposite is observed. The maximum value of κ_T is higher than that of pure water.

For the 2 m solutions, at temperatures above 273 K, the magnitude of κ_T is further reduced compared to that of the 1 m solutions (see the right panels of Figure 3). But the trends observed in the effects exerted by specific ions at 1 m also hold at 2 m, with a few exceptions. For the chloride salts, the extent of the reduction of κ_T is again correlated with the valency of the ions, as observed at 1 m. The drop of κ_T is higher for divalent ions, but the difference between the κ_T in the $MgCl_2$ and $CaCl_2$ solutions is somewhat larger than that observed at 1 m. All sulfate salts have a similar κ_T in this temperature regime, also in keeping with the trends observed at 1 m. K_2SO_4 represents a notable exception, with a somewhat larger κ_T than the remaining sulfate salts. Focusing now on the dependence of κ_T on temperature, the variation of κ_T at temperatures between 273–300 K is quite mild for all salts. Indeed, except for $MgCl_2$ and $CaCl_2$, the results

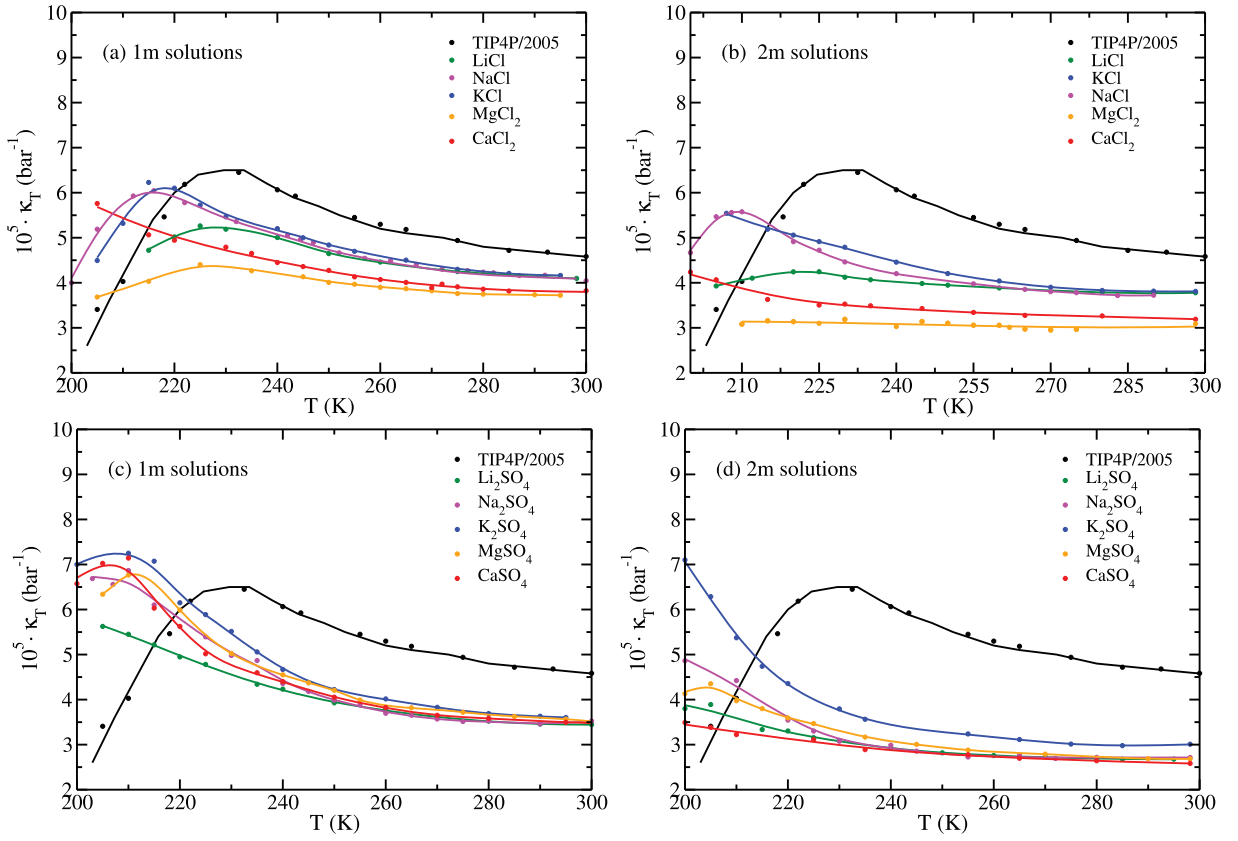

Figure 3. Isothermal compressibility of aqueous electrolyte solutions at 1 m (left) and 2 m (right) as a function of temperature along the 1 bar isobar, as calculated in MD simulations using the Madrid-2019 force-field. The top panels show results for chloride salts and the bottom panels for sulfate salts.

can be coherent with a scenario in which κ_T reaches a minimum in this temperature range, although further simulations are needed to confirm this. Note that the minimum of κ_T in pure TIP4P/2005 water is estimated to occur at about 310 K [47]. Our results suggest high concentrations of salt might shift the minimum to lower temperatures.

For the 2 m solutions and temperatures below 273 K, κ_T retains its anomalous behaviour, with κ_T increasing as temperature lowers for all the salts. For the chlorides, maxima are only observed for NaCl and LiCl. In both solutions, the maximum in κ_T is further shifted lo lower temperatures in comparison with that of the 1 m solution. As for the sulfates, $MgSO_4$ is the only salt that retains the maximum in κ_T, which is shifted again to lower temperatures and adopts a lower height than in the 1 m solution. The case of K_2SO_4 is also quite remarkable, as it exhibits a rather steep increase as temperature approaches 200 K.

Unfortunately, we are not aware of many experimental results on the isothermal compressibility of salt solutions. We only found some data for a few salts (NaCl, $MgCl_2$ $NaSO_4$ and $MgSO_4$), restricted to temperatures above 273 K [70]. The values of κ_T obtained with the Madrid-2019 model are compared to experimental measurements in Table 2. As can be seen, the Madrid-2019 model correctly reproduces the drop in κ_T when salt is added, and the magnitude of κ_T is also rather close to the experimental data, with relative differences lower than about 5%. Remarkably, the Madrid-2019 force-fields predicts the right order in which those salts reduce κ_T as compared to experiments, with NaCl exhibiting the largest value of κ_T and Na_2SO_4 the lowest value of κ_T (see Table 2). Additionally, experiments predict a mild variation of κ_T with temperature within 273 K–318 K, which is also consistent with the results of the simulations.

3.3. Water self-diffusion coefficient in salt solutions

The self-diffusion of water in the solutions (D) is reported with respect to the self-diffusion of pure water (D_0) at the same thermodynamic conditions, represented as D/D_0. The TIP4P/2005 model provides a reliable estimate of water diffusion at room conditions, leading to a slight underestimation of the experimental results (or a 1% overestimation when finite-size effects are taken into account) [8,72]. In this work, we evaluated the water

Table 2. Comparison of the isothermal compressibility for some salt solutions at room pressure and at 273 K as measured in experiments [70] and obtained with the Madrid-2019 force-field. The experimental concentration of each solution is shown in parentheses in the first column. The experimental value of κ_T pure water is taken from Ref. [71].

	$10^5\ \kappa_T$ (bar^{-1})		
System	Exp.	Madrid-2019	%Err
Pure water	5.09	5.00	1.8
NaCl (1.0615 m)	4.40	4.29	2.5
$MgCl_2$ (0.9837 m)	4.01	3.79	5.5
$MgSO_4$ (0.9247 m)	3.84	3.74	2.6
Na_2SO_4 (1.0020 m)	3.64	3.54	2.7

diffusion constant down to 200 K. The mean square displacement (MSD) of water for some selected temperatures is shown in Figure 4(a). As reported in previous work [60], at the lower temperatures three regions can be differentiated in the evolution of MSD with time. Between the ballistic and diffusive regime, there is a stage in which the MSD remains constant for some time, reflecting that water molecules reside for some time within cages formed by its neighbours before reaching the diffusive regime. This caging is also present in the salt solutions (although in some cases it occurs at shorter times than those used to calculate the MSD). Figure 4 clearly shows that the times from which the slope was measured (larger than 2 ns for T > 215 K and than 10 ns for T < 215 K) is in the diffusive regime and it is not affected by caging.

Only the diffusive regime was taken into account to calculate the diffusion constant from the Einstein relation Equation (3). As can be seen in Figure 5, TIP4P/2005 successfully captures the experimentally observed reduction of the diffusion constant by up to four orders of magnitude from room temperature to 200 K. TIP4P/2005 provides estimates of D_0 somewhat higher than the experimental values below 240 K. But, in general, it can be derived that using TIP4P/2005 for water ensures that the scaling of D with respect to D_0 does not introduce a significant error due to a poor prediction of D_0, nor does it mask a potential cancellation of errors between D and D_0.

3.3.1. Dependence of D/D_0 on salt concentration

The effect of salt concentration on the diffusion of water for the chloride salts at ambient conditions is shown in Figure 6, together with experimental data [75]. The Madrid-2019 force-field tends to overestimate the effect of salt concentration for all the chloride salts, but it succeeds in predicting the correct order of the magnitude of the slowing effect exerted by different ions. The order, from the strongest to the weakest effect, is consistent between experiments and simulations: $MgCl_2$, $CaCl_2$, LiCl and NaCl. The exception is KCl that, according to experiments, slightly increases the diffusion coefficient of water, but simulations predict a slight deceleration. As shown in Ref. [34], better agreement with experiments is likely to be found using a $+0.75e$ scaled charge (instead of $+0.85e$ as in the Madrid-2019 force-field used in this work). However, that deteriorates the prediction of thermodynamic properties, and that it is the reason why the Madrid-2019 force-field was chosen in this study. In any case, the predictions are significantly better than those obtained using force-fields with integer charges [34,40], and even with some polarisable models [28]. Unfortunately, we have not been able to find a similar experimental study on the effect of salt concentration on water dynamics for sulfate salts. Previous work has shown that at ambient conditions the Madrid-2019 force field predicts that for sulfate salts the effect of the cation is less relevant than in the chlorides, finding that water diffusion is rather similar for all sulfate salt solutions when compared at the same concentration [40]. Finally, the D/D_0 ratios for systems with 4440 water molecules and the corresponding number of ions for achieving 1 m and 2 m concentrations of NaCl are displayed in Figure 6, showing that the size effects of water's relative diffusion are insignificant, thereby validating the main conclusions of this work.

3.3.2. Dependence of D/D_0 on temperature in NaCl solutions

The effect of temperature on the self-diffusion of water in a 1 m NaCl solution is shown in Figure 7, which compares the results of the Madrid-2019 force field with experimental data [76]. Experimental measurements indicate that the effect of NaCl on the diffusion of water changes with temperature, and below a certain temperature, it actually facilitates the diffusion of water. The Madrid-2019 model qualitatively reproduces this temperature dependence, but the temperature at which NaCl starts to enhance the diffusion of water is significantly lower in the simulations ($T \sim 245$ K) compared to the experiments by Garbacz *et al.* [76] ($T \sim 295$ K). Notably, at the lowest temperature at which experiments were performed ($T \sim 230$ K), a 1 m NaCl solution can increase the diffusion of water by a factor of two. Simulations with the Madrid-2019 model indicate that the enhancement of water diffusion becomes more pronounced as temperature decreases. The diffusion coefficient of water increases by more than a factor of 3 at 210 K.

To gain further insight on the effect of temperature on water diffusion, the ratio D/D_0 as a function of NaCl concentration at different temperatures is shown in Figure 8. According to our simulations, at the two highest shown temperatures ($T = 298.15$ K and $T = 255$ K), D/D_0

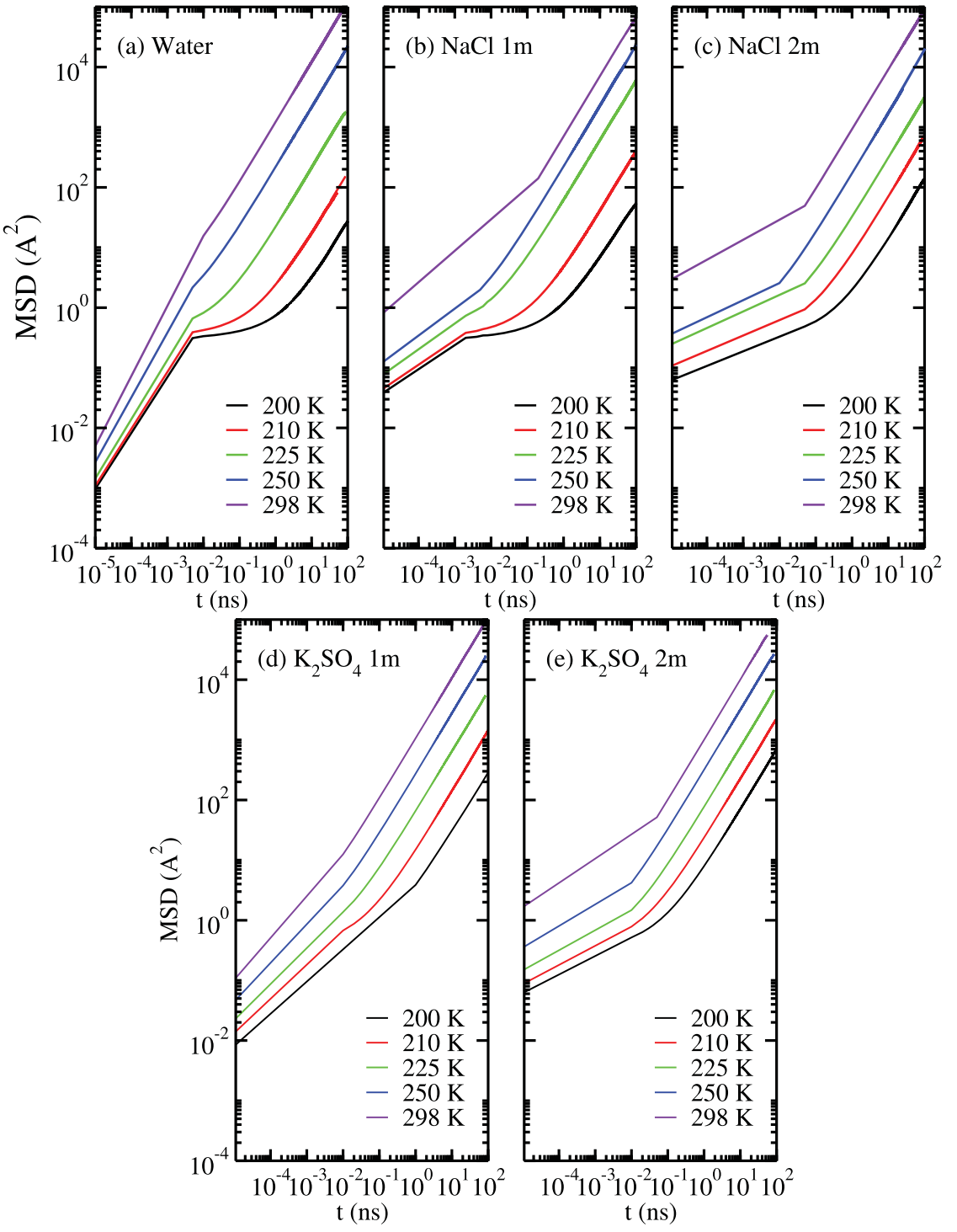

Figure 4. Mean square displacement at 1 bar for water TIP4P/2005 water, NaCl and K_2SO_4 solutions at 1 and 2 m as a function of time.

decreases monotonically as salt concentration increases up to a 4 m concentration. However, at lower temperatures, D/D_0 initially increases until it reaches a maximum at moderate concentration (between $\sim$1–1.5 m, depending on the temperature), beyond which it falls again. At $T = 225$ K, D/D_0 falls below one at high salt concentrations, indicating that adding salt concentrations above 3.5 m leads to a reduction of water diffusion. An analogous plot built using a fit to experimental data given in Ref. [76] is shown in the lower panel of Figure 8. As can be seen, simulations reproduce qualitatively the experimental results, but the agreement is

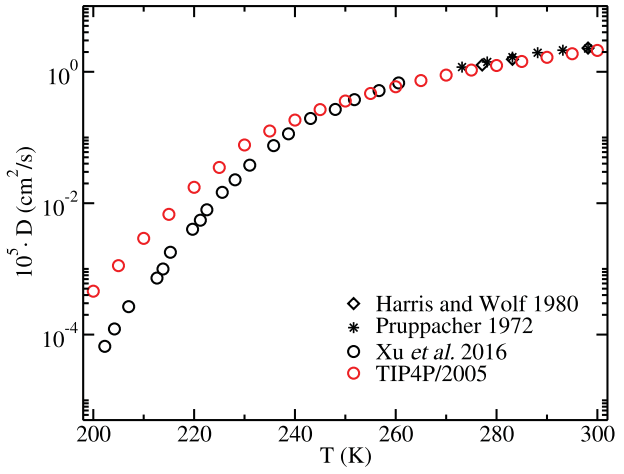

Figure 5. Diffusion coefficient for TIP4P/2005 water as a function of temperature at room pressure (this work) compared to experiments from Refs. [24,73,74].

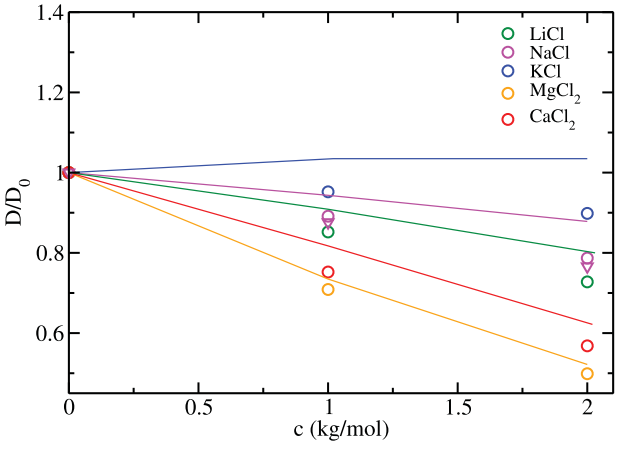

Figure 6. Ratio of the self-diffusion of water in chloride solutions (D) to the self-diffusion of pure water (D_0) at 298.15 K as a function of salt concentration. Down-triangles represent the ratios obtained for NaCl with systems containing 4440 water molecules instead of 555 (circles). Experimental data (solid lines) are taken from Ref. [75].

not quantitative. As already mentioned in the Introduction, the transition from 'structure maker' to 'structure breaker' of NaCl has already been reported in a previous simulation study using TIP5P and a force field with integer charges for the ions [27]. Our simulation agree qualitatively with those findings.

3.3.3. Dependence of D/D_0 on temperature in chloride solutions

The water self-diffusion coefficient as a function of temperature for 1 and 2 m chloride and sulfate solutions at ambient pressure is shown in Figure 9. The more striking result is that all the considered chloride and sulfate

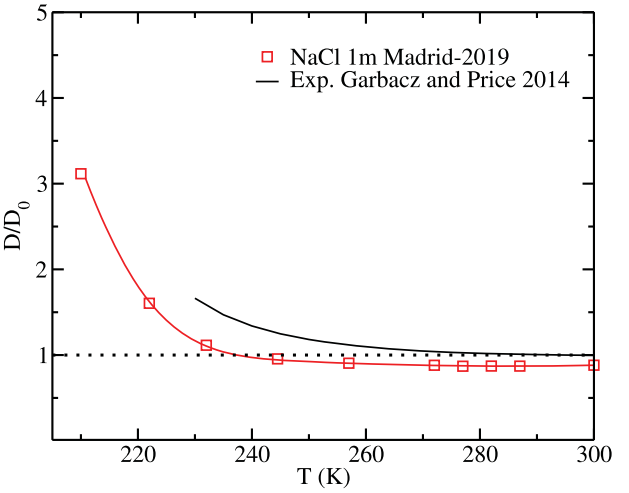

Figure 7. Ratio of the self-diffusion coefficient of water in 1 m NaCl solutions to the self-diffusion of pure water (D/D_0) as a function of temperature at room pressure for the Madrid-2019 force-field and from a fit to experimental data taken from Ref. [76].

salts lead to an increase of water diffusion at low temperatures both in the 1 m and 2 m solutions. The factor by which the diffusion increases is different for each salt.

As can be seen in Figure 9(a), at 1 m all chloride salts, except for $MgCl_2$, enhance water diffusion by a factor of about 4–5 at temperatures around 210 K. $MgCl_2$ is less efficient in enhancing water diffusion, leading to a increase by a factor of 2. The crossover from the reduction to the enhancement of water diffusion occurs at different temperatures depending on the cation. It is observed that cations retain the same order when classified according to the factor by which they reduce water mobility at ambient conditions down to temperatures of about 230 K. Indeed, the temperature at which the crossover takes place follows this same order. However, at lower temperatures, there are several crossings between the curves of different salts. In chloride solutions, the efficiency of the various cations to reduce the coefficient diffusion of water at room conditions does not correlate with its efficiency to increase it at very low temperatures.

When the concentration increases from 1 m to 2 m, chloride salts further hinder water diffusion in the higher temperature regime. The crossover from water diffusion reduction to enhancement occurs at somewhat lower temperatures than in the 1 m solutions. In general, all the salts produce a similar increase at the lowest temperatures at the two concentrations. The exceptions are KCl that leads to a larger rise in water diffusion in the 2 m than in the 1 m solution, and $MgCl_2$ for which an enhancement of water mobility does not occur at the considered temperatures.

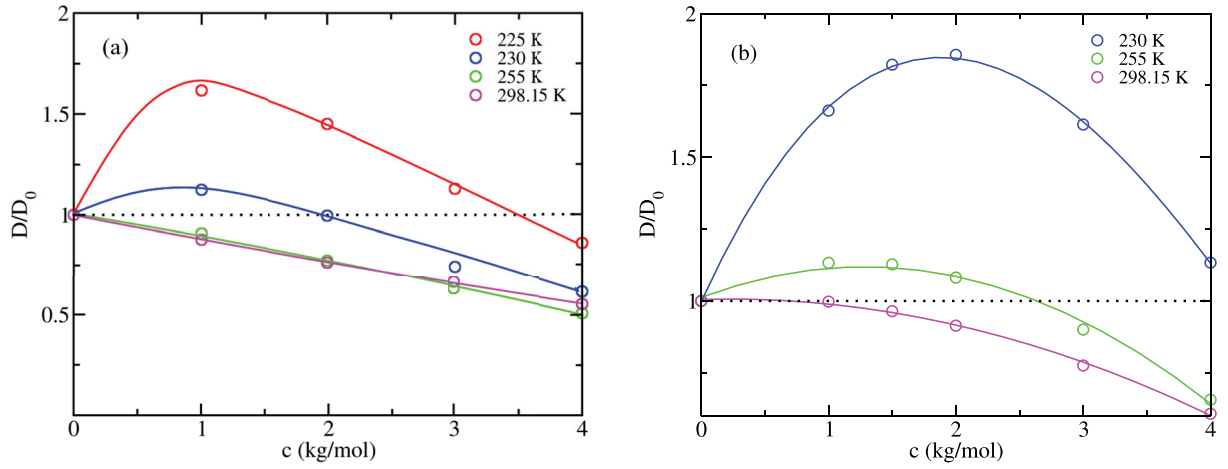

Figure 8. D/D_0 for NaCl solutions as a function of concentration for different isotherms at room pressure. Solid lines are a guide for the eye. (a) simulations with the Madrid-2019 force field, (b) fits to experimental data taken from Ref. [76].

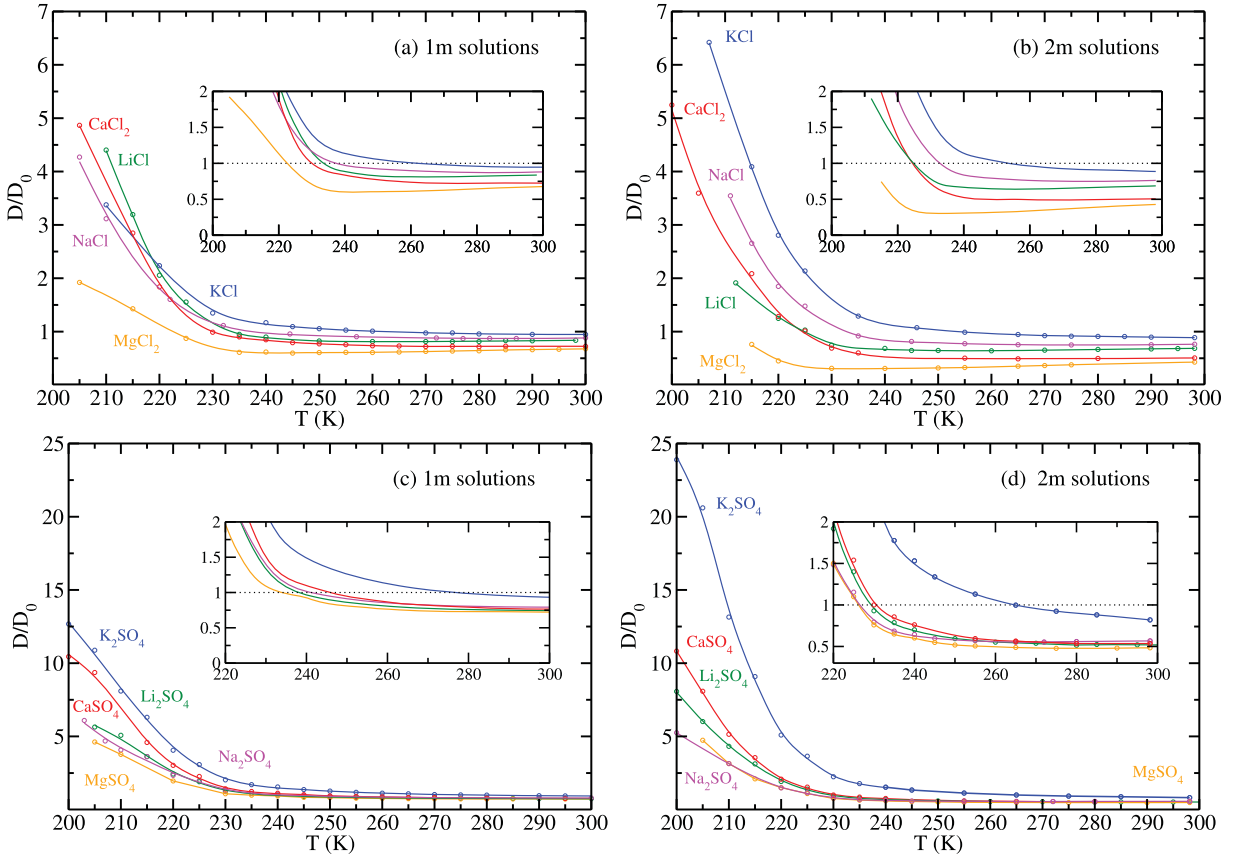

Figure 9. Self-diffusion of water in salt solutions relative to self-diffusion of pure water (D/D_0) as a function of temperature at room pressure. Chloride solutions at (a) 1 m and (b) 2 m, and sulfate solutions at (c) 1 m and (d) 2 m. Insets show enlarged views to better visualise the crossing from reduction ($D/D_0 < 1$) to increase ($D/D_0 > 1$) of water diffusion coefficient. The dotted line marks $D/D_0 = 1$.

3.3.4. Dependence of D/D_0 on temperature in sulfate solutions

As shown in Figure 9 sulfate salts lead to a significantly higher enhancement of water diffusion at lower temperatures than in the corresponding chloride salts. This is specially notable for K_2SO_4 and $CaSO_4$, which increase water diffusion coefficient by a factor of about 12 and 10, respectively, at 200 K. This enhanced diffusion constant is already visible from the MSD graphs shown in Figure 4. Except for K_2SO_4, all the sulfate solutions reduce water movement by a similar factor at room temperature. K_2SO_4, however, hardly modifies water mobility at room

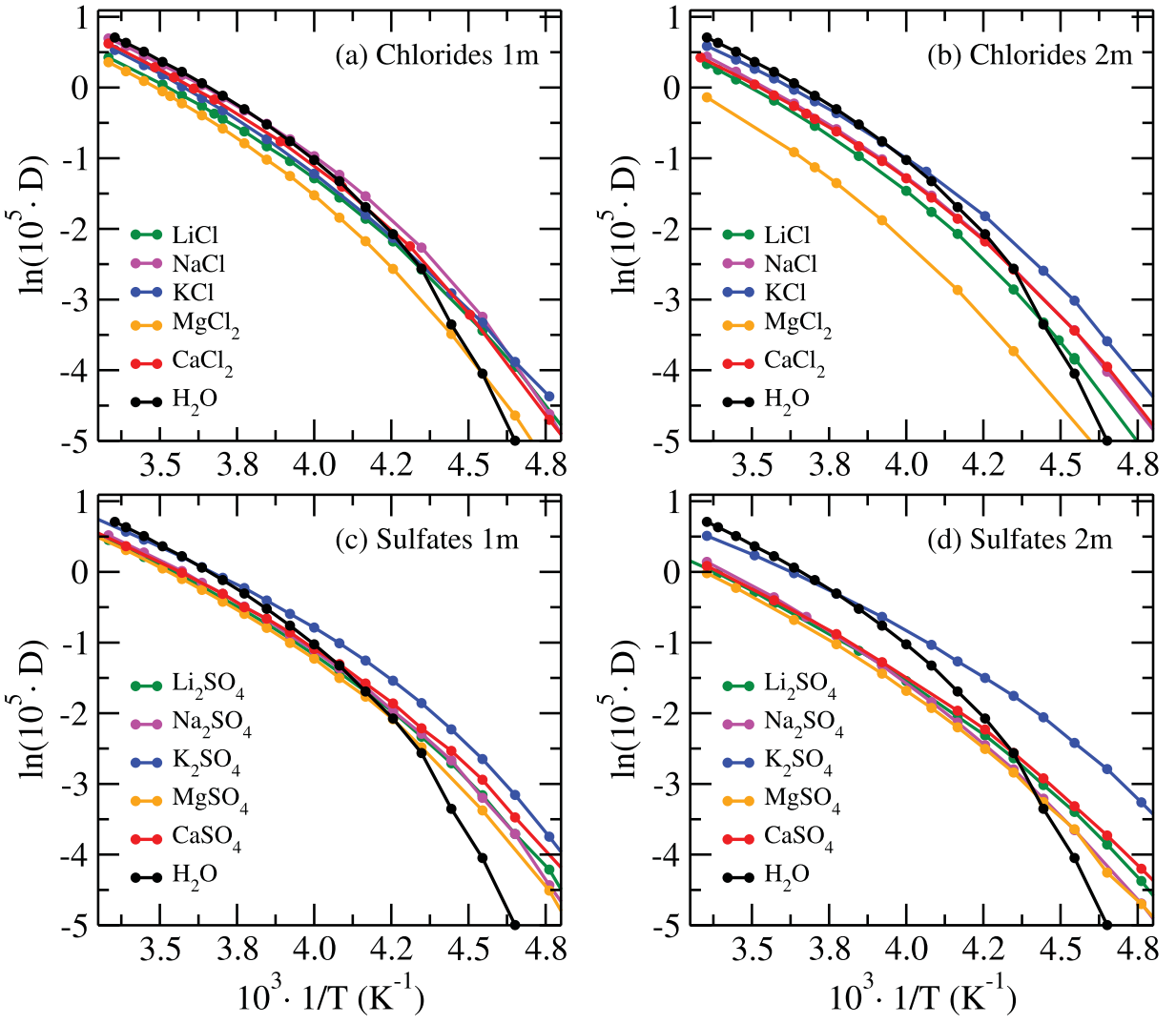

Figure 10. Self-diffusion of water (in $cm^{2/s}$) as a function of inverse temperature at room pressure. (a) Chloride solutions at (a) 1 m and (b) 2 m, and sulfate solutions at (c) 1 m and (d) 2 m.

temperature but is very efficient at increasing D/D_0 in the supercooled solution. The crossover from a reduction to an increase of water diffusion coefficient occurs at temperatures around 240–250 K for all the cations, except again for K_2SO_4 for which the crossover occurs already at around 280 K.

The main trends observed for the 1 m sulfate solutions still hold for the 2 m solutions, except for a few differences. All the cations reduce water mobility by a similar factor at room temperature, except for K_2SO_4 which again is significantly less efficient in reducing water mobility than the rest of the salts. All the salts, except K_2SO_4, are almost coincident down to about 260 K. Below this temperature, the effect of each salt starts to slightly differ, and the crossover from the reduction to the enhancement of water diffusion occurs at temperatures within 230 K–225 K depending on the salt, which is about 10–15 K lower than in the 1 m solution. The factor by which they accelerate water at 200 K is somewhat larger than that observed at 1 m. The behaviour of K_2SO_4 is again distinctly different from the remaining cations. For sulfates at 1 m the crossover from reduced to increased water diffusion constant occurs at significantly higher temperatures ($T > 265$ K) and below this temperature K_2SO_4 becomes really efficient and at 200 K increases water diffusion by a factor close to 25.

It is important to keep in mind that even though simulations predict that salt increases water mobility in the supercooled solution, the self-diffusion coefficient of water at those temperatures is 4–5 orders of magnitude lower than at room conditions. Thus, even adding the more efficient salt in enhancing water movement (K_2SO_4 which increases D/D_0 by a factor of 25), the diffusion of water is still very low at these temperatures.

3.3.5. Arrhenius plot of water self-diffusion in salt solutions

The effect of temperature on the self-diffusion of pure water is often represented using an Arrhenius plot that allows to identify dynamic transitions from Arrhenius to super-Arrhenius behaviour [77]. At high temperature (typically above 270 K), water diffusion follows Arrhenius law [77,78] and can be fitted to the following expression:

$$D = A \exp\left(-\frac{E_a}{RT}\right) \tag{4}$$

where A is a fitting parameter and E_a is the activation energy. At moderate super-cooling the dynamic behaviour is well represented by Mode Coupling Theory of glass dynamics, but as supercooling increases, there is a transition to Arrhenius behaviour characterised by an activation energy associated to hopping [79].

The logarithm of water self-diffusion as a function of the inverse temperature is shown in Figure 10. From this plot it becomes evident that whereas at high temperature the diffusion coefficient of water is higher in pure water than in salt solutions, in the deeply supercooled regime the diffussion coefficient of water is smaller in pure water than in salt solutions for all the solutions considered in this work (for the 2 m $MgCl_2$ this is also true but the crossing occurs at lower temperatures). Thus, without any exception, at low temperatures, the presence of a salt accelerates the dynamics of water in contrast to the behaviour exhibited at high temperatures. It is also interesting to note that water diffusion in most of the salt solutions exhibits a rather linear behaviour at high temperatures, which is indicative of Arrhenius behaviour, consistent with previous findings [28]. At moderate supercooling there is a deviation from linearity, which is again recovered at high supercooling. It would be interesting to locate the dynamic transitions in the salt solutions, but a proper identification would require extending the simulations both in the high and low temperature regime. We leave this analysis for further work.

4. Conclusions

To summarise, we have performed an exhaustive simulation study using the Madrid-2019 force-field on the effect of chloride and sulfate salts on the anomalous behaviour of supercooled water, focusing on the isothermal compressibility and on the water self-diffusion coefficient. One of the main conclusions of this work is that the anomalous behaviour in the isothermal compressibility is still present in these salt solutions (at least up to a 2 m concentration), and that almost all salts are able to enhance the diffusion coefficient of water in the highly supercooled regime. A more extensive study was performed for the 1 m NaCl solution, which includes simulations at different pressures, and that allowed us to locate the LLCP from the convergence of the lines of maximum isothermal compressibility and maximum heat capacity. The LLCP is shifted to slightly higher temperatures and lower pressures than in pure TIP4P/2005 water. Another important finding is that addition of salt induces an enhancement of water mobility of almost all salts in the highly supercooling regime. This effect is specially significant in the K_2SO_4 solution. However, it is important to keep in mind that this study is performed at 1 m and 2 m concentrations, which significantly surpass the solubility of this salt at room pressure which is only of about 0.65 m at room temperature and pressure [80]. In any case, the experimental verification of the effect on adding small concentrations of K_2SO_4 on enhancing water diffusion in the high supercooled regime would be of great interest.

Unfortunately, there are not much experimental measurements on salts under supercooled conditions which can be used to test the predictions of the model. In that sense, we hope that this work will stimulate further work on the experimental side. If a salt is found that shifts the LLCP to higher temperatures and the homogeneous nucleation line to lower temperatures, this might provide an opportunity to experimentally observe the LLCP.

Comparison of the effect of the various salts on the shifts on the TMDs and on the isothermal compressibility reveals a certain correlation between both properties. At 1 m, $CaCl_2$ does not exhibit a maximum in κ_T within the considered temperature range, which is consistent with the fact that this chloride salt is the one resulting in a larger shift of the TMD to lower temperatures. With a few exceptions, the 2 m solutions do not exhibit (for the temperatures considered in this work, namely above 200 K) a maximum in κ_T, which is consistent with a larger shift in the TMD to lower temperatures than in the 1 m solutions. Note, however, that correlation between both properties is far from being perfect. For example, it is surprising that Li_2SO_4 TMD occurs at relatively high temperatures, but it does not exhibit a maximum in κ_T. Correlations between the behaviour of the isothermal compressibility and density, and the self-diffusion of water are even harder to identify. But given that previous work have found a correlation between the region where structural and dynamic anomalies occur in supercooled water [81], it is likely that some correlation also exists in supercooled salt solutions.

In future work, it would be interesting to perform a detailed microscopic analysis to try to explain the different behaviours depending on the salt added. In particular, we aim to understand why different salts produce different shifts in the isothermal compressibity and why some

salts and more efficient than others in increasing the self-diffusion coefficient of water in the highly supercooled regime.

The influence of José Luis Abascal on this work and our scientific careers can hardly be overemphasised. Besides being one of the leading authors in the proposal of TIP4P/2005 and Madrid-2019 force fields, he has also contributed to the evaluation of the Widom line and the properties of supercooled water for TIP4P/2005, which served as inspiration for this work. With his optimistic personality and his ever availability to lend a hand to anyone knocking on his door, we feel privileged to share many wonderful times with him. We learnt recently (Liquid Matter Conference 2024, Mainz) about some recent experimental work leaded by Prof. Caupin showing that NaCl reduces the viscosity of water at low temperatures, a behavior fully consistent with the predictions of this work. "From structure-maker to structure-breaker: Viscosity of supercooled NaCl solutions", Jan Eichler, Johannes Stefanski, Florian Schulz, Bruno Issenmann, and Frédéric Caupin.

Disclosure statement

No potential conflict of interest was reported by the author(s).

Funding

This project has been funded by the Agencia Estatal de Investigación [grant numbers PID2022-136919NB-C31 and PID2020-115722GB-C21]. L. F. S. thanks Ministerio de Educación y Formación Profesional (MEFP) for a predoctoral Formacion Profesorado Universitario [grant number FPU22/02900].

ORCID

L. F. Sedano http://orcid.org/0000-0002-1394-6263
C. Vega http://orcid.org/0000-0002-2417-9645
E. G. Noya http://orcid.org/0000-0002-6359-1026

References

[1] C.A. Angell, J. Shupper and J.C. Tucker, J. Phys. Chem. **77**, 3092 (1973). doi:10.1021/j100644a014
[2] J.R. Speedy and C.A. Angell, J. Chem. Phys. **65**, 851–858 (1976). doi:10.1063/1.433153
[3] P.H. Poole, F. Sciortino, U. Essmann and H.E. Stanley, Nature **360**, 324 (1992). doi:10.1038/360324a0
[4] T.E. Gartner III, L. Zhang, P.M. Piaggi, R. Car, A.Z. Panagiotopoulos and P.G. Debenedetti, Proc. Natl. Acad. Sci. **117**, 26040 –26046 (2020). doi:10.1073/pnas.2015440117.
[5] O. Mishima, L.D. Calvert and E. Whalley, Nature **314**, 76 (1985). doi:10.1038/314076a0
[6] O. Mishima and H.E. Stanley, Nature **396**, 329–335 (1998). doi:10.1038/24540
[7] S. Woutersen, B. Ensing, M. Hilbers, Z. Zhao and A. Angell, Science **359**, 1463–1472 (2018). doi:10.1126/science.aao7049
[8] J.L.F. Abascal and C. Vega, J. Chem. Phys. **123**, 234505 (2005). doi:10.1063/1.2121687
[9] J.L.F. Abascal, E. Sanz, R. Garcia and C. Vega, J. Chem. Phys. **122**, 234511 (2005). doi:10.1063/1.1931662
[10] L. Zhang, H. Wang, R. Car and E. Weinan, Phys. Rev. Lett. **126**, 236001 (2021). doi:10.1103/PhysRevLett.126.236001
[11] T.E. Gartner, L. Zhang, P.M. Piaggi, R. Car, A.Z. Panagiotopoulos and P.G. Debenedetti, Proc. Natl. Acad. Sci. **117**, 26040 (2020). doi:10.1073/pnas.2015440117
[12] P.G. Debenedetti, F. Sciortino and G.H. Zerze, Science **369**, 289–292 (2020). doi:10.1126/science.abb9796
[13] J. Weis, F. Sciortino, A.Z. Panagiotopoulos and P.G. Debenedetti, J. Chem. Phys. **157**, 024502 (2022). doi:10.1063/5.0099520
[14] J.R. Espinosa, J.L.F. Abascal, L.F. Sedano, E. Sanz and C. Vega, J. Chem. Phys. **158**, 244505 (2023). doi:10.1063/5.0147345
[15] F. Sciortino, I.T.E. Garner and P.G. Debenedetti, J. Chem. Phys. **160**, 104501 (2024). doi:10.1063/5.0196964
[16] K.H. Kim, K. Amann-Winkel, N. Giovambattista, A. Späh, F. Perakis, H. Pathak, M.L. Parada, C. Yang, D. Mariedahl, T. Eklund, T.J. Lane, S. You, S. Jeong, M. Weston, J.H. Lee, I. Eom, M. Kim, J. Park, S.H. Chun, P.H. Poole and A. Nilsson, Science **370** (6519), 978–982 (2020). doi:10.1126/science.abb9385
[17] S. Chatterjee and P.G. Debenedetti, J. Chem. Phys. **124**, 154503 (2006). doi:10.1063/1.2188402
[18] O. Mishima, J. Chem. Phys. **126**, 244507 (2007). doi:10.1063/1.2743434
[19] M.P. Longinotti, M.A. Carignano, I. Szleifer and H.R. Corti, J. Chem. Phys. **134**, 244510 (2011). doi:10.1063/1.3602468
[20] D. Corradini, P. Gallo and M. Rovere, J. Phys. Condens. Matter **22**, 284104 (2010). doi:10.1088/0953-8984/22/28/284104
[21] T. Yagasaki, M. Matsumoto and H. Tanaka, J. Chem. Phys. **150**, 214506 (2019). doi:10.1063/1.5096429
[22] D. Corradini, P. Gallo and M. Rovere, J. Chem. Phys. **132**, 134508 (2010). doi:10.1063/1.3376776
[23] L. Perin and P. Gallo, J. Phys. Chem. B **127**, 4613–4622 (2023). doi:10.1021/acs.jpcb.3c00703
[24] Y. Xu, N.G. Petrik, R.S. Smith, B.D. Kay and G.A. Kimmel, Proc. Natl. Acad. Sci. **113**, 14921 (2016). doi:10.1073/pnas.1611395114
[25] W.S. Price, H. Ide and Y. Arata, J. Phys. Chem. A **103**, 448 (1999). doi:10.1021/jp9839044
[26] Y. Ni, N.J. Hestand and J.L. Skinner, J. Chem. Phys. **126**, 191102 (2018). doi:10.1063/1.5029822
[27] J.S. Kim and A. Yethiraj, J. Phys. Chem. B **112**, 1729–1735 (2008). doi:10.1021/jp076710+
[28] J.S. Kim, Z. Wu, A.R. Morrow, A. Yethiraj and A. Yethiraj, J. Phys. Chem. B **116**, 12007–12013 (2012). doi:10.1021/jp306847t
[29] Y. Ding, A.A. Hassanali and M. Parrinello, Proc. Natl. Acad. Sci. **111**, 3310–3315 (2014). doi:10.1073/pnas.1400675111
[30] Z.R. Kann and J.L. Skinner, J. Chem. Phys. **141**, 104507 (2014). doi:10.1063/1.4894500

[31] I.V. Leontyev and A.A. Stuchebrukhov, J. Chem. Phys. **130**, 085102 (2009). doi:10.1063/1.3060164

[32] I.V. Leontyev and A.A. Stuchebrukhov, J. Chem. Theory Comput. **6**, 3153–3161 (2010). doi:10.1021/ct1002048

[33] I.V. Leontyev and A.A. Stuchebrukhov, Phys. Chem. Chem. Phys. **13**, 2613–2626 (2011). doi:10.1039/c0cp01971b

[34] S. Blazquez, M.M. Conde and C. Vega, J. Chem. Phys. **158**, 054505 (2023). doi:10.1063/5.0136498

[35] S. Blazquez, J.L.F. Abascal, J. Lagerweij, P. Habibi, P. Dey, T.J.H. Vlugt, O.A. Moultos and C. Vega, J. Chem. Theory Comput. **19**, 5380–5393 (2023). doi:10.1021/acs.jctc.3c00562

[36] Y. Yao, M.L. Berkowitz and Y. Kanai, J. Chem. Phys. **134**, 184507 (2011). doi:10.1063/1.3589419

[37] Y. Yao, M.L. Berkowitz and Y. Kanai, J. Chem. Phys. **143**, 241101 (2015). doi:10.1063/1.4938083

[38] M.L. Berkowitz, J. Phys. Chem. B **125**, 13069–13076 (2021). doi:10.1021/acs.jpcb.1c08383

[39] I. Zeron, J.L.F. Abascal and C. Vega, J. Chem. Phys. **151**, 134504 (2019). doi:10.1063/1.5121392

[40] S. Blazquez, M.M. Conde, J.L.F. Abascal and C. Vega, J. Chem. Phys. **156**, 194505 (2022). doi:10.1063/5.0093643

[41] L.F. Sedano, S. Blazquez, E.G. Noya, C. Vega and J. Troncoso, J. Chem. Phys. **156** (15), 154502 (2022). doi:10.1063/5.0087679

[42] F. Gámez, L.F. Sedano, S. Blazquez, J. Troncoso and C. Vega, J. Molec. Liq. **377**, 121433 (2023). doi:10.1016/j.molliq.2023.121433

[43] C.P. Lamas, C. Vega and E.G. Noya, J. Chem. Phys. **156**, 134503 (2022). doi:10.1063/5.0085051

[44] D. Biriukov, H.-W. Wang, N. Rampal, C. Tempra, P. Kula, J.C. Neuefeind, A.G. Stack and M. Předota, J. Chem. Phys. **156**, 194505 (2022). doi:10.1063/5.0093643

[45] N.V.S. Avula, M.L. Klein and S. Balasubramanian, J. Phys. Chem. Lett. **14**, 9500–9507 (2023). doi:10.1021/acs.jpclett.3c02112

[46] A.Z. Panagiotopoulos and S. Yue, J. Phys. Chem. B **127**, 430–437 (2023). doi:10.1021/acs.jpcb.2c07477

[47] H.L. Pi, J.L. Aragones, C. Vega, E.G. Noya, J.L. Abascal, M.A. Gonzalez and C. McBride, Molec. Phys. **107**, 365–374 (2009). doi:10.1080/00268970902784926

[48] J.L.F. Abascal and C. Vega, J. Chem. Phys. **133**, 234502 (2010). doi:10.1063/1.3506860

[49] J.L.F. Abascal and C. Vega, J. Chem. Phys. **134**, 186101 (2011). doi:10.1063/1.3585676

[50] M.A. González and J.L.F. Abascal, J. Chem. Phys. **132**, 096101 (2010). doi:10.1063/1.3330544

[51] B. Hess, C. Kutzner, D. van der Spoel and E. Lindahl, J. Chem. Theory Comput. **4**, 435–447 (2008). doi:10.1021/ct700301q

[52] S. Nosé, Molec. Phys. **52**, 255–268 (1984). doi:10.1080/00268978400101201

[53] W.G. Hoover, Phys. Rev. A **31**, 1695–1697 (1985). doi:10.1103/PhysRevA.31.1695

[54] M. Parrinello and A. Rahman, J. Appl. Phys. **52** (12), 7182–7190 (1981). doi:10.1063/1.328693

[55] T. Darden, D. York and L. Pedersen, J. Chem. Phys. **98**, 10089–10092 (1993). doi:10.1063/1.464397

[56] U. Essmann, L. Perera, M.L. Berkowitz, T. Darden, H. Lee and L.G. Pedersen, J. Chem. Phys. **103**, 8577–8592 (1995). doi:10.1063/1.470117

[57] M.P. Allen and D.J. Tildesley, *Computer Simulations of Liquids* (Oxford Science Publications, Oxford, 1987).

[58] B. Hess, H. Bekker, H.J.C. Berendsen and J.G.E.M. Fraaije, J. Chem. Phys. **18**, 1463–1472 (1997).

[59] J.P. Ryckaert, G. Ciccotti and H.J.C. Berendsen, J. Comp. Phys. **23**, 327–341 (1977). doi:10.1016/0021-9991(77)90098-5

[60] V. Teboul and A.P. Kerasidou, Molec. Phys. **45**, 304–309 (2019). doi:10.1080/08927022.2018.1505045

[61] M. Fushiki, Phys. Rev. E **68**, 021203 (2003). doi:10.1103/PhysRevE.68.021203

[62] I.C. Yeh and G. Hummer, J. Phys. Chem. B **108**, 15873–15879 (2004). doi:10.1021/jp0477147

[63] D. Liu, Y. Zhang, C.-C. Chen and S.-H. Chen, Proc. Natl. Acad. Sci. **104**, 9570–9574 (2007). doi:10.1073/pnas.0701352104

[64] P.S.Z. Rogers and K.S. Pitzer, J. Phys. Chem. Ref. Data **11**, 15 (1982). doi:10.1063/1.555660

[65] C. Vega, M.M. Conde, C. McBride, J.L.F. Abascal, E.G. Noya, R. Ramirez and L.M. Sesé, J. Chem. Phys. **132**, 046101 (2010). doi:10.1063/1.3298879

[66] R.A. Fine and F.J. Millero, J. Chem. Phys. **63**, 89 (1975). doi:10.1063/1.431070

[67] R. Lebermand and A.K. Soper, Nature **378**, 364–366 (1995). doi:10.1038/378364a0

[68] J. Holzmann, R. Ludwig, A. Geiger and D. Pacheck, Angew. Chem. Int. Ed **46**, 8907–8911 (2007). doi:10.1002/anie.v46:46

[69] C. Zhang, S. Yue, A.Z. Panagiotopoulos, M.L. Klein and X. Wu, Nat. Commun. **13**, 882 (2022).

[70] F.J. Millero, G.K. Ward, F.K. Lepple and E.V. Hoff, J. Chem. Phys. **78** (16), 1636–1643 (1974). doi:10.1021/j100609a008

[71] G.S. Kell, J. Chem. Eng. Data **15**, 119 (1970). doi:10.1021/je60044a003

[72] O.A. Moultos, I.N. Tsimpanogiannis, A.Z. Panagiotopoulos and I.G. Economou, J. Phys. Chem. B**118**, 5532–5541 (2014). doi:10.1021/jp502380r

[73] K.R. Harris and L.A. Woolf, J.C.S. Faraday I **76**, 377–385 (1980). doi:10.1039/f19807600377

[74] H.R. Pruppacher, J. Chem. Phys. **56**, 101–107 (1972). doi:10.1063/1.1676831

[75] K.J. Müller and H.G. Hertz, J. Phys. Chem. **100** (4), 1256–1265 (1996). doi:10.1021/jp951303w

[76] P. Garbacz and W.S. Price, J. Phys. Chem. A **118**, 3307 (2014). doi:10.1021/jp501472s

[77] I.N. Tsimpanogiannis, O.A. Moultos, L.F.M. Franco, M.B.M. de Spera, M. Erdös and I.G. Economou, Molec. Sim. **45**, 425–453 (2019). doi:10.1080/08927022.2018.1511903

[78] L. Xu, F. Mallamace, Z. Yan, F.W. Starr, S.V. Buldyrev and H.E. Stanley, Nat. Phys. **5**, 565–569 (2009). doi:10.1038/nphys1328

[79] M. De Marzio, G. Camisasca, M. Rovere and P. Gallo, J. Chem. Phys. **144**, 074503 (2016). doi:10.1063/1.4941946

[80] P. Song and Y. Yao, Calphad **27**, 343 (2003). doi:10.1016/j.calphad.2004.02.001

[81] J.R. Errington and P.G. Debenedetti, Nature **409**, 318 (2001). doi:10.1038/35053024